Atmos. Chem. Phys. Discuss., 11, 12725–12762, 2011
www.atmos-chem-phys-discuss.net/11/12725/2011/
doi:10.5194/acpd-11-12725-2011

Atmospheric Chemistry and Physics Discussions

Observations of hydroxyl and peroxy radicals and the impact of BrO at Summit, Greenland in 2007 and 2008

J. Liao[1], L. G. Huey[1], D. J. Tanner[1], S. Brooks[2], J. E. Dibb[3], J. Stutz[4], J. L. Thomas[4,*], B. Lefer[5], C. Haman[5], and K. Gorham[6]

[1]School of Earth and Atmospheric Sciences, Georgia Institute of Technology, Atlanta, Georgia, USA
[2]NOAA Atmospheric Turbulence and Diffusion Division, TN, USA
[3]Climate Change Research Center, Institute for the Study of Earth, Oceans and Space, University of New Hampshire, Durham, NH, USA
[4]University of California Los Angeles, Department of Atmosphere Ocean Science, Los Angeles, CA, USA
[5]Department of Geosciences, University of Houston, TX, USA
[6]Chemistry, University of California, Irvine, California, USA
[*]now at: UPMC Univ. Paris 06; Université Versailles St-Quentin; CNRS/INSU, UMR 8190; LATMOS-IPSL, Paris, France

Received: 6 April 2011 – Accepted: 13 April 2011 – Published: 26 April 2011

Correspondence to: L. G. Huey (greg.huey@eas.gatech.edu)

Published by Copernicus Publications on behalf of the European Geosciences Union.

Abstract

The Greenland Summit Halogen-HO_x (GSHOX) Campaign was performed in spring 2007 and summer 2008 to investigate the impact of halogens on HO_x (=OH + HO_2) cycling above the Greenland Ice Sheet. Chemical species including hydroxyl and peroxy radicals (OH and HO_2 + RO_2), ozone (O_3), nitrogen oxide (NO), nitric acid (HNO_3), nitrous acid (HONO), reactive gaseous mercury (RGM), and bromine oxide (BrO) were measured during the campaign. The median midday values of HO_2 + RO_2 and OH concentrations observed by chemical ionization mass spectrometry (CIMS) were 2.7×10^8 molec cm^{-3} and 3.0×10^6 molec cm^{-3} in spring 2007, and 4.2×10^8 molec cm^{-3} and 4.1×10^6 molec cm^{-3} in summer 2008. A basic photochemical 0-D box model highly constrained by observations of H_2O, O_3, CO, CH_4, NO, and J values predicted HO_2 + RO_2 ($R = 0.90$, slope = 0.87 in 2007; $R = 0.79$, slope = 0.96 in 2008) reasonably well and under predicted OH ($R = 0.83$, slope = 0.72 in 2007; $R = 0.76$, slope = 0.54 in 2008). Constraining the model to HONO observations did not significantly change the predictions. Including bromine chemistry in the model constrained by observations of BrO improved the correlation between observed and predicted HO_2 + RO_2 and OH, and brought the average hourly OH and HO_2+RO_2 predictions closer to the observations. These model comparisons confirmed our understanding of the dominant HO_x sources and sinks in this environment and indicated that BrO impacted the OH levels at Summit. Although, significant discrepancies between observed and predicted OH could not be explained by the measured BrO. Finally, observations of enhanced RGM were found to be coincident with under prediction of OH.

1 Introduction

Summit, Greenland (72°34′ N, 38°29′ W, alt = 3.3 km) is located in the middle of the Greenland Ice Sheet and has been the site of a series of scientific studies beginning with ice coring in the 1980s (e.g. Hammer et al., 1980; Mayewski and Bender, 1995).

ACPD
11, 12725–12762, 2011

In more recent years, the interaction between photochemically active species in the snowpack and the overlying atmosphere has been studied in detail at Summit and other polar stations (e.g. Dibb et al., 1997; Grannas et al., 2007; Jones et al., 2008; Davis et al., 2001; Huey et al., 2004). Elevated levels of species emitted from surface snow such as NO, CH_2O, and H_2O_2 have been observed over sunlit snow in a series of campaigns (Dibb et al., 2002, 2004; Honrath et al., 1999, 2002; Hutterli et al., 1999, 2001, 2004; Davis et al., 2001; Slusher et al., 2002; Helmig et al., 2008). Snowpack emissions of radical sources (HONO, H_2O_2, and CH_2O) and NO_x have the potential to significantly enhance HO_x photochemistry in these locations (e.g. Yang et al., 2002; Chen et al., 2001).

The hydroxyl radical (OH) and peroxy radicals ($HO_2 + RO_2$) have been measured in a few polar locations and the concentrations vary based on the radical sources as well as environmental conditions. The daytime mean value of OH observed at Palmer station (64°46′ S, 64°3.0′ W) in Antarctica was 3×10^5 molec cm^{-3}in austral summer (Jefferson et al., 1998). The low OH levels were found to be consistent with the high solar zenith angle, extensive cloud coverage and low NO_x levels (typical near detection limits of 2–4 pptv) (Jefferson et al., 1998). OH concentrations observed at South Pole were unexpectedly high, with an average value of 2.0 ($\pm$0.9) $\times 10^6$ molecule cm^{-3} in November and December from three field campaigns ISCAT 98, ISCAT 00 and ANTCI 03 (Mauldin et al., 2001, 2004, 2010; Grannas et al., 2007). The high OH levels at South Pole were due to snowpack emissions that gave high levels of NO_x and to a lesser extent formaldehyde (Davis et al., 2001; Hutterli et al., 2004). A photochemical model constrained to CH_2O and H_2O_2 measurements predicted OH levels with a median modeled to observed (*M/O*) ratio of 1.27 (Chen et al., 2004). However, the *M/O* ratio for OH was found to vary with NO levels at South Pole (Chen et al., 2001, 2004). The model over predicted OH significantly at low NO (NO < 50 pptv; *M/O* > 1.5) and high NO (NO > 150 pptv; *M/O* = 1.5) levels but agreed better at moderate levels of NO (Chen et al., 2004). Sjostedt et al. (2007) measured OH (mean 6.3×10^6 molec cm^{-3}) and $HO_2 + RO_2$ (mean 2.8×10^8 molec cm^{-3}) levels at Summit,

ACPD
11, 12725–12762, 2011

Greenland during summer 2003. The observed $HO_2 + RO_2$ levels agreed well with the model predictions, although the measured OH levels were elevated compared to the predictions (Sjostedt et al., 2007; Chen et al., 2007). Sjostedt et al. (2007) suggested that halogen may be present at Summit, perturbing the HO_x cycling and enhancing OH levels. In contrast, a later study at Halley Bay, Antarctica (75°35′ S, 26°19′ W) found average OH levels of 3.9×10^5 molec cm^{-3} in February with typical maximum (local noontime) levels of 7.9×10^5 molec cm^{-3} (Bloss et al., 2007, 2010). The OH levels at Halley Bay were slightly higher than measured at Palmer station in the same season of the year but significantly lower than observed at South Pole. The low levels of OH were surprising as mean diurnal NO levels of up to ~14 pptv and significant IO and BrO levels of up to ~7 pptv and ~9 pptv were observed. A photochemical box model including halogen reactions significantly over predicted observed levels of OH and HO_2, although the model well predicted the mean levels and diurnal patterns of NO_x (NO and NO_2) (Bloss et al., 2007, 2010). The mean daily maximum *M/O* ratio of OH was 3.8 and of HO_2 was 2.8. The mean observed HO_2 to OH ratio of 46 was in good agreement with the mean predicted value of 44 from the model considering bromine and iodine chemistry, and no elevated OH was observed.

Prior to the GSHOX campaign, there was only indirect evidence that BrO may exist at Summit, Greenland. Although the overall reservoir of bromine at Summit is much less than in the coastal Arctic where ODEs are typically observed, vertical profiles of ozone obtained from balloon borne sensors have demonstrated that ozone in the boundary layer is consistently depleted relative to the air above (Helmig et al., 2002). However, the reaction of NO (~20 pptv) and RO_2 (~10^8 molec cm^{-3}) in the boundary layer at Summit should give a local ozone production of ~2 ppbv day^{-1} (Sjostedt et al., 2007). This type of ozone production is evident in the NO_x($NO + NO_2$) rich South Pole boundary layer (Crawford et al., 2001) where boundary layer ozone is elevated relative to the air above (Helmig et al., 2002). In addition, mercury oxidation in snow has been observed at Summit, Greenland (Faïn et al., 2008; Brooks et al., 2011). As $Br + Hg^0(GEM) \rightarrow Hg^{2+}(RGM)$ is the only well established reaction that can initiate

ACPD
11, 12725–12762, 2011

such rapid conversion of GEM to RGM (Ariya et al., 2002; Donohoue et al., 2006), depleted GEM and elevated RGM may be a signature of active bromine chemistry.

High levels (up to 30–40 pptv) of BrO are typically found in the polar marine boundary layer near large sources of halides during ODEs (Tuckermann et al., 1997; Hausmann et al., 1994; Saiz-lopez et al., 2007; Liao et al., 2011a). However, significant levels of BrO have been observed in a variety of other marine locations. For example, BrO was observed in the tropical marine boundary layer within the Cape Verde archipelago by Read et al. (2008) with an average daytime level of 2.5 pptv. Up to ~7 pptv of BrO was observed in the mid-latitude marine boundary at Roscoff, France (48.7° N, 4.0° W) (Mahajan et al., 2009) and at the Mace Head Atmospheric Research Station, Ireland (53.33° N, 9.90° W) (Saiz-lopez et al., 2006).

To investigate the hypothesis that BrO is present at Summit and that it impacts HO_x photochemistry, a suite of instruments were used to measure OH, $HO_2 + RO_2$, BrO and other species at Summit, Greenland in spring 2007 and summer 2008. The observations of OH and $HO_2 + RO_2$, and their comparison to photochemical models are presented in this paper. The BrO observations and the associated snowpack chemistry are discussed by Stutz et al. (2011) and Thomas et al. (2010), respectively.

2 Methods

A comprehensive collection of instruments were used at Summit, Greenland during May–June 2007 and June–July 2008 to measure trace gases and radicals, aerosols, actinic fluxes, and meteorological parameters. Table 1 provides a summary of the measurements during the campaign. The details of measurement techniques not specifically summarized are presented in the references in Table 1. Most of the measurements were located in a satellite camp ~1 km to the south of the main station. The layout of the experiment is shown in Fig. 1.

ACPD
11, 12725–12762, 2011

2.1 HO_x measurement by CIMS

The chemical ionization mass spectrometry (CIMS) instrument to measure HO_x (OH and sum of $HO_2 + RO_2$) is nearly identical to that used to measure HO_x in 2003 (Sjostedt et al., 2007; Sjostedt et al., 2006). The basic methods are based on the work of Tanner et al. (1997). The CIMS was located in the satellite camp (Fig. 1) and the inlet was about 1.5 m above the snow surface. The dominant uncertainty in the OH and $HO_2 + RO_2$ measurements is the accuracy of the calibration source (Sjostedt et al., 2007). The combined uncertainties are estimated to be ~30% for OH measurements and ~35% for $HO_2 + RO_2$ measurements. The calibration standards for both OH and HO_2 measurements are produced from the photolysis of ambient water vapor, consequently, the uncertainty in the ratio of observed OH to $HO_2 + RO_2$ is smaller than the absolute uncertainties.

2.2 BrO measurement by CIMS

The CIMS used to measure BrO levels at Summit is essentially identical to the low pressure CIMS systems used to measure halogens on the NASA DC-8 and NOAA P3 aircrafts during the ARCTAS and ARCPAC campaigns (Neuman et al., 2010), and at Barrow, Alaska during the OASIS 2009 campaign (Liao et al., 2011a). The details of the instrument and air sampling inlet are described in (Liao et al., 2011a) and only significant differences are described here.

SF_6^- was used as a reagent ion to ionize BrO and other species such as SO_2.

$$SO_2 + SF_6^- \rightarrow F_2SO_2^- + SF_4 \quad \text{(R1)}$$

$$BrO + SF_6^- \rightarrow BrO^- + SF_6 \quad \text{(R2)}$$

$$Br_2 + SF_6^- \rightarrow Br_2^- + SF_6 \quad \text{(R3)}$$

The charge transfer reaction of SF_6^- with BrO Reaction (R2) was observed for the first time as part of this work. The rate constant for this reaction was determined relative

ACPD
11, 12725–12762, 2011

to that of SF_6^- with Br_2 Reaction (R3) (Streit, 1982). BrO was synthesized from the reaction of O (^3P) with Br_2 in excess ozone as described in Liao et al. (2011a). The ratio of the rate constant for Reaction (R3) to Reaction (R2) was determined to be 1.0 ± 25% in the laboratory. The rate constant for Reaction (R2) derived from this work is $(5 \pm 2) \times 1\,0^{-10}$ molec cm^{-3} s^{-1}.

SO_2 was used as our primary calibration gas for determining the sensitivity of the CIMS system in the field (Kim et al., 2007; Slusher et al., 2001) and as a proxy to track the sensitivity of BrO. The ratio of the sensitivity of BrO to that of SO_2 was determined in the laboratory after the campaign as a function of dew point (dewpt). The average sensitivity of SO_2 was ~4 Hz pptv^{-1} in 2007 and ~60 Hz pptv^{-1} in 2008 summit campaign. The sensitivity ratio of SO_2 to BrO was determined as Eq. (1)

$$\frac{SO_2}{BrO} = \begin{cases} 0.76 - 0.096 \times \text{dewpt} - 0.00154 \times \text{dewpt} & (\text{dewpt} > -35\,^{\circ}\text{C}) \\ 2.2 & (\text{dewpt} < -35\,^{\circ}\text{C}). \end{cases} \quad (1)$$

The background signal level of BrO during the 2007 Summit campaign was determined by periodically scrubbing the sampled air with an active carbon filter, similar to that used before for removal of SO_2, HO_2NO_2, and HNO_3. In 2008 the background was determined by using glass wool because it was found to effectively remove halogen species (Neuman et al., 2010).

The detection limits of BrO measurements are estimated to be ~1.8 pptv in 2007 and ~0.7 pptv in 2008. Considering the uncertainty in SO_2 standard concentration (~10%), the uncertainties in the sensitivity ratios between BrO and Br_2(~25%) and between Br_2 and SO_2 (~5%), the total uncertainty in BrO measurements is estimated to be ~36%. The concentrations of BrO at Summit in spring 2007 and summer 2008 were often near the detection limits of both instruments (detection limit of LP DOAS = 0.5–2 pptv; detection limit of CIMS = ~1–2 pptv). Moreover, the measurements of BrO at Summit were the earliest applications of CIMS to measure ambient BrO. SF_6^- was used as the reagent ion to detect BrO at that time. After these campaigns the more selective reagent ion, I^-, was found to sensitively detect BrO (Neuman et al., 2010). In

ACPD
11, 12725–12762, 2011

addition, the capability of CIMS, using I^-, to accurately and sensitively measure BrO was demonstrated in Liao et al. (2011a). Moving forward, CIMS observations of BrO with I^- are preferred to SF_6^- as the latter ion is more prone to interferences as it is more reactive (Huey et al., 1995). Consequently, conclusions drawn from the CIMS BrO observations in this study must be considered in the context of potential interferences.

2.3 BrO measurement by DOAS

The primary BrO measurement during the Summit campaign was a long path differential absorption spectrometer (LP DOAS). The techniques of the LP DOAS instrument were based on the work of Stutz and Platt (1997). The LP DOAS measured BrO over a path of either 2 km or 5/4 (2007/2008) km. The optical paths were 1.5–3 m above the snow. The LP DOAS telescope was located at the edge of the clean air boundary in the south of the station and two reflectors were located 2 km and 5/4 (2007/2008) km to the South of the light source (Fig. 1). The details of BrO measurement by LP DOAS are provided by Stutz et al. (2011).

2.4 Mercury measurement

Tekran models 2537a/1130/1135 (Brooks et al., 2008) were used to measure gaseous elemental mercury (GEM), reactive gaseous mercury (RGM), also known as gaseous oxidized mercury (GOM), and fine particle mercury (FPM). The details of the mercury measurements are described in the work of Brooks et al. (2011).

2.5 Actinic fluxes measurement

Actinic Fluxes were measured by a Scanning Actinic Flux Spectrometer (SAFS) (Shetter et al., 1999) by University of Houston. The photolysis rate coefficients (J values) of atmospheric compounds were calculated based on the sum of downwelling and upwelling Actinic Fluxes.

ACPD
11, 12725–12762, 2011

2.6 Photochemical models

A 0-Dimensional steady-state HO_x-NO_x-CH_4 model is used to evaluate the HO_x chemistry at Summit. The model is identical to that described in Sjostedt et al. (2007) and is denoted as the base model (BM). The BM involves 46 chemical reactions which include 8 photolysis reactions and is constrained by the measurements of photolysis rate coefficients (J values) and the following gases: H_2O, O_3, CO, CH_4, and NO. The input data used to constrain the model were averaged to a 10 minute basis. The model predictions are compared to OH and $HO_2 + RO_2$ measurements (assuming RO_2 is primarily CH_3O_2). The rate constants are taken from the JPL compilation (Sander et al., 2006), and the J values are derived from the measured actinic fluxes (Shetter et al., 1999). Similar to the work of Sjostedt et al. (2007), the model can be run either constrained or unconstrained to HONO measurements. This allows evaluation of the impact of HONO on HO_x levels and the radical budget. The model constrained to HONO observations is referred as BM_HONO.

To examine the impact of BrO on HO_x levels, bromine reactions (see Table 2) were added to the BM. The model incorporating the bromine chemistry is referred as BM_BrO. Reaction (R6) (in Table 2) acts as a source of HO_x. HOBr serves as a temporary reservoir of HO_x and heterogeneous loss of HOBr is effectively a loss of HO_x. HOBr levels were assumed to be in steady-state and controlled by Reactions (2, 8, 9) (in Table 2). This assumption was found to be reasonable by Liao et al. (2011b). This allowed predictions of OH and $HO_2 + RO_2$ when BrO measurements were available.

One significant difference from the work of Sjostedt et al. (2007) is that observations of CH_2O and H_2O_2 were not available. For this reason, the BM was used to predict CH_2O and H_2O_2 levels. In order to test the ability of the model to calculate these species, predictions of CH_2O and H_2O_2 using data from the 2004 Summit campaign were compared to observations. Both CH_2O and H_2O_2 predictions are in reasonable agreement with the measurements (CH_2O: $R = 0.68$, mean $M/O = 1.3$; H_2O_2: $R = 0.72$, mean $M/O = 2.4$), which suggests that the steady state model is viable for estimation

ACPD
11, 12725–12762, 2011

of CH_2O and H_2O_2 within about a factor of two. The impact of this relatively high uncertainty in mixing ratios of CH_2O and H_2O_2 on predictions of HO_x and its partitioning are discussed in Sect. 4.2.

3 Results

3.1 OH and ($HO_2 + RO_2$) observations

The time series of observations of OH, $HO_2 + RO_2$, $J(O^1D)$, BrO, NO, HNO_3, HONO, O_3, RGM, temperature, wind speeds and wind directions on a 10 min time base in spring 2007 and summer 2008 are shown in Fig. 2. The observations of OH and $HO_2 + RO_2$ were filtered to exclude the periods when NO >50 pptv. High NO mixing ratios at Summit are almost always due to pollution plumes from the station power generator. High NO dramatically brought down the $HO_2 + RO_2$ concentrations and raised the OH concentrations (Fig. 3). Similar phenomena were observed by previous works as well (e.g. Sjostedt et al., 2007; Bloss et al., 2007). The HO_x instrument was shut down to save reagent gases at night (22:00–06:00 Western Greenland Standard Time (WGST)) when the OH concentrations decreased to near detection limit (10^5 molec cm^{-3}). The gaps in the data other than night time and high NO periods are due to instrument maintenance or malfunction.

Diurnal profiles of OH and $HO_2 + RO_2$ largely followed the patterns of $J(O^1D)$ with a maximum at local noon, consistent with the behaviors of short-lived photochemically active species. Although 24 h of daylight are present in summer time at Summit, $J(O^1D)$ decreased by approximately a factor of 100 from noon to midnight. The maxima mid-day levels of OH and $HO_2 + RO_2$ increased as temperature, $J(O^1D)$ and O_3 increased, which were consistent with the previous finding that O^1D reacting with H_2O and snow emissions of H_2O_2 were the dominant HO_x sources at Summit (Chen et al., 2007) (Mid-day is defined as 10:00–15:00 WGST). Overall, the maximum mid-day OH and $HO_2 + RO_2$ concentrations increased during the measurement period in

ACPD
11, 12725–12762, 2011

spring 2007 as the summer solstice was approached. There was no significant trend in the maximum mid-day OH and $HO_2 + RO_2$ concentrations during summer 2008 (12 June 2008–8 July 2008) as the measurement period was centered about the solstice. The average mid-day OH and $HO_2 + RO_2$ concentrations were higher in summer 2008 than that in spring 2007, likely a result of the higher radiative fluxes and dew points in summer time. The midday median ratio of $HO_2 + RO_2$ to OH was 107:1 in spring 2007 and 102:1 in summer 2008 and the midday mean ratio of $HO_2 + RO_2$ to OH was 109:1 in spring 2007 and 108:1 in summer 2008. The $HO_2 + RO_2$ to OH ratios are comparable to other measurements performed in the lower troposphere in mid latitudes (Ren et al., 2008). The mid-day median and mean values of OH and $HO_2 + RO_2$ observations, as well as $J(O^1D)$, $J(NO_2)$, NO, HNO_3, HONO, O_3, BrO, RGM and temperature in spring 2007 and summer 2008 are summarized in Table 3.

3.2 NO, HNO_3 and HONO observations

Diurnal profiles of NO and HONO were also observed at Summit. The average mid-day concentrations of NO and HONO were ~12 pptv and ~6 pptv, respectively. HONO levels were obtained from measurements of soluble nitrite (NO_2^-) from the mist chamber (Dibb et al., 2002). However, it should be noted that the derived HONO levels must be considered an upper limit to gas phase HONO as other species might also produce nitrite in solution. Due to the increase of the boundary layer height through the day, the diurnal profiles of NO had a local minimum at noon (Thomas et al., 2010). Elevated HNO_3 was observed by mist chamber during the days when photochemically enhanced NO was observed. Higher NO, HNO_3 and HONO concentrations were observed in spring 2007 than in summer 2008.

3.3 RGM and GEM observations

Up to ~250 pg m^{-3} RGM were observed in spring 2007 campaign. Clear diurnal profiles of RGM were observed when RGM was greater than 100 pg m^{-3}. Because bromine atoms are one of the few established species that efficiently converts GEM

ACPD
11, 12725–12762, 2011

into RGM (Ariya et al., 2002; Donohoue et al., 2006), elevated RGM peaks indicated that significant levels of BrO may be present. Higher RGM levels were observed in spring 2007 than in summer 2008, which suggests that the concentrations of BrO at Summit might be higher in spring 2007 than in summer 2008. High RGM appeared to coincide with high NO and HNO_3 in most cases. This is consistent with snow photochemistry activating bromine chemistry as described in Thomas et al. (2010).

3.4 BrO observations

BrO mixing ratios detected by the LP DOAS ranged from below detection limit to 5.5 pptv with an average value of 1.6 pptv in 2007 at Summit. BrO was also measured by CIMS in the later period of the 2007 campaign with a mean value of 1.7 pptv, ranging from below detection limit to 6.4 pptv. Lower BrO mixing ratios were observed by both LP DOAS ($[BrO]_{mean}$ = 0.9 pptv for all data available) and CIMS ($[BrO]_{mean}$ = 1.5 pptv for all data available) in summer 2008. BrO mixing ratios in 2008 generally ranged from below detection limit to 4 pptv and 5 pptv detected by LP DOAS and CIMS respectively. To be noted, the BrO concentrations at Summit were often near detection limits of both instruments. Diurnal patterns of BrO were observed in spring 2007 and the early part (10 June to 13 June) of summer 2008 by the CIMS with maximum concentrations in the daytime, which is consistent with BrO as a photochemically active product. No significant diurnal patterns of BrO were observed by the CIMS in the later period of summer 2008 as the daytime BrO levels were near the detection limit.

ACPD
11, 12725–12762, 2011

4 Discussion

4.1 Model comparison

4.1.1 Base Model (BM)

The predicted OH and $HO_2 + RO_2$ from the BM are plotted against the observations in Fig. 4. Note that, the discrepancy between HO_x observations and predictions increased at high wind speeds and blowing snow periods, which is consistent with the observations in Sjostedt et al. (2007). Therefore, the OH and $HO_2 + RO_2$ data at high wind speeds ($WS > 8\,m\,s^{-1}$) were excluded from the comparisons. Overall, the observed and predicted OH and $HO_2 + RO_2$ from the BM were well correlated ($HO_2 + RO_2$: $R = 0.90$, OH: $R = 0.83$ in 2007; $HO_2 + RO_2$: $R = 0.79$, OH: $R = 0.76$ in 2008). The BM well predicted the magnitude of $HO_2 + RO_2$ and under predicted OH, especially in summer 2008 ($HO_2 + RO_2$: slope = 0.87, OH: slope = 0.72 in 2007; $HO_2 + RO_2$: slope = 0.96, OH: slope = 0.54 in 2008). The slopes were given by equally weighted bivariate regressions. The model predicted an average midday $HO_2 + RO_2$ to OH ratio of 121:1 in 2007 and 125:1 in 2008, consistent with the values predicted by Chen et al. (2007) using input data from the summit 2003 campaign. The observed average midday $HO_2 + RO_2$ to OH ratios were 109:1 in 2007 and 108:1 in 2008. This indicates that the BM model captures the dominant sources and sinks of HO_x, even with the lack of H_2O_2 and CH_2O observations and the exclusion of halogen chemistry. However, enhanced OH levels relative to the base model predictions were observed.

4.1.2 Base Model constrained to HONO measurements (BM_HONO)

The correlation coefficients and slopes between predictions from the BM_HONO and observations are shown in Fig. 5 ($HO_2 + RO_2$: $R = 0.84$, slope = 0.90 in 2007 and $R = 0.79$, slope = 1.09 in 2008; OH: $R = 0.78$, slope = 0.92 in 2007 and $R = 0.78$, slope = 0.72 in 2008). The slopes were given by equally weighted bivariate

ACPD
11, 12725–12762, 2011

regressions. In 2007, the average modeled to observed (*M/O*) ratios of $HO_2 + RO_2$ and OH were 0.87 and 0.84 from the BM, and were 1.18 and 1.25 from the BM_HONO. In 2008, the average *M/O* ratios of $HO_2 + RO_2$ and OH were 1.06 and 0.87 from the BM, and were 1.22 and 1.05 from the BM_HONO. The predictions of HO_x from the BM_HONO were slightly higher than that from the BM. However, inclusion of HONO source in the model did not improve the ratio of OH to $HO_2 + RO_2$ relative to the observations. As constraining to HONO in the model does not improve the correlation between predictions and observations significantly and the observed HONO may have interference from other compounds, the BM is preferred for comparison to HO_x levels in this environment.

4.1.3 Model incorporating halogen chemistry (BM_BrO)

To investigate the impact of BrO on HO_x, predicted OH and $HO_2 + RO_2$ from the BM_BrO unconstrained by HONO measurements and constrained by BrO measurements from the CIMS (BM_BrO_{CIMS}) and LP DOAS (BM_BrO_{LPDOAS}) in 2007 and 2008 are also plotted against the observations (Fig. 6). Overall, the correlation between the observed and predicted OH and $HO_2 + RO_2$ were slightly improved (increased 0.03 except $HO_2 + RO_2$ in 2007) by incorporation of bromine chemistry with the BrO constrained to the CIMS observations. Predicted OH increased 12% $([OH]_{pred\_BrO\_CIMS}/[OH]_{pred})_{avg}$ in 2007 and 10% in 2008, and predicted $HO_2 + RO_2$ decreased 10% in 2007 and 8% in 2008 on average when the BM_BrO was constrained to CIMS BrO. Predicted OH increased 10% in 2007 and 4% in 2008, and predicted $HO_2 + RO_2$ decreased 8% in 2007 and 3% in 2008 on average when the BM_BrO was constrained to LP DOAS BrO. These results indicate that BrO impacted the concentrations of OH and $HO_2 + RO_2$ at Summit, although all of the enhancement in observed OH relative to model predictions cannot be explained by the influence of BrO.

ACPD
11, 12725–12762, 2011

4.2 Impact of H_2O_2 and CH_2O

Because CH_2O and H_2O_2 were not observed, they had to be predicted with the photochemical model which may lead to under estimation of them as they are emitted to the atmosphere from the snowpack (Hutterli et al., 1999 and 2001). Under estimation of CH_2O and H_2O_2 results in under prediction of OH and $HO_2 + RO_2$, but does not significantly impact the ratios of OH/ $HO_2 + RO_2$. For example, a 30% increase in the model production rate of H_2O_2 or CH_2O would increase HO_x levels by ~5% and ~10% but would impact the ratio of OH to RO_2 by less than 2%. According to the study of HO_x at Summit in 2003 by Chen et al. (2007), H_2O_2 is the largest snow emitted HO_x sources at Summit, contributing to 37% of the net HO_x sources compared to only 3% from CH_2O. As snow emissions of H_2O_2 increase with temperature (Chen et al., 2007), the warmer temperature in summer 2008 may have contributed to the lower correlation between predicted and observed HO_x in that year. For this reason, temperature dependent snow emissions of H_2O_2, based on net snow-air exchange rate = $A \times \exp(B/\text{Temperature}_{\text{snow}}) - C \times [H_2O_2]$ (A, B and C are adjustable constants; temperature is assumed to be ambient temperature instead of snow temperature) (Chen et al., 2007), were added to the BM. No significant improvement of the correlation was found between predicted and observed HO_x. However, as observations of H_2O_2 and CH_2O were not carried out in 2007 or 2008, enhanced snow photochemistry producing these and potentially other radical precursors in 2008 cannot be ruled out.

4.3 Average comparison

Figure 7 shows the average diurnal profiles of hourly OH and $HO_2 + RO_2$ concentrations from observations and predictions from the BM and the BM_BrO constrained to CIMS measurements in 2007 and 2008. The error bars of the observations are the overall uncertainties including the measurement uncertainties and ambient fluctuations. The error bars of the predictions are the propagated uncertainties from the model inputs uncertainties and variations. The BM simulated the concentrations of OH and

ACPD
11, 12725–12762, 2011

$HO_2 + RO_2$ within the combined uncertainties, except for the OH concentrations in the late afternoons in summer 2008. The BM also under predicts the OH concentrations in both 2007 and 2008. The midday median modeled to observed (*M/O*) ratio of OH was 0.88 and 0.87 in 2007 and 2008, and the midday median *M/O* ratio of $HO_2 + RO_2$ was 0.97 and 1.08 in 2007 and 2008. A low *M/O* ratio of OH was also reported in Sjostedt et al. (2007). The average hourly $HO_2 + RO_2$ and OH predictions from the BM_BrO constrained to CIMS BrO measurements in 2007 slightly over estimated their concentrations due to the absence of CIMS BrO measurements in the early period of the 2007 campaign. The OH concentrations predicted from BM_BrO were higher compared to the results from the BM, and the average hourly predicted $HO_2 + RO_2$ concentrations slightly decreased when BM incorporated bromine chemistry in 2008. The model including bromine chemistry brought the predictions both of OH and $HO_2 + RO_2$ closer to the observations in 2008. The impact of bromine chemistry on $HO_2 + RO_2$ concentrations was smaller than on OH concentrations. The box model consistently under predicts the OH concentrations in the later afternoons, which indicates that box model underestimates the sources of OH as the radiation flux and boundary layer height decrease. A similar behavior was observed by Sjostedt et al. (2007). However, the 1-D model reasonably predicts OH concentrations in the later afternoon (Thomas et al., 2011). The photochemical box model is constrained to limited measurements (e.g. NO) and assumes that the gas species are homogeneously distributed. The slightly different vertical locations (~1 m apart in the vertical dimension) of the inlets for the HO_x (~1.5 m) and NO (~2.5 m) instruments and the steeper vertical gradient of NO levels in the later afternoon (Thomas et al., 2010) may contribute to but cannot account for all the under predictions of OH by the box model. Snow emitted compounds with higher concentrations or steeper vertical gradients in the later afternoon not included in the photochemical box model may contribute to the under predictions of OH and impact the photochemistry at Summit in the later afternoon.

ACPD
11, 12725–12762, 2011

4.4 Enhanced OH and RGM

Due to the limitations of BrO measurements discussed earlier, observations of RGM were also investigated as a proxy for bromine and potentially other chemistry. The correlations between the BM predictions and observations of HO_x were examined for enhanced RGM levels (gray dots in Fig. 8) and low RGM levels (black dots in Fig. 8). Enhanced RGM levels were taken to be >45 pg m^{-3} ([RGM]$_{avg\_2007}$ = 45 pg m^{-3}) in 2007 and >11 pg m^{-3} ([RGM]$_{avg\_2008}$ = 11 pg m^{-3}) in 2008.

When high RGM periods were excluded, the slope between the predicted and observed OH significantly increased: the slope of OH increased from 0.72 to 0.97 in 2007 and increased from 0.54 to 0.85 in 2008. The slopes were given by equally weighted bivariate regressions. The correlation between the predicted and observed OH and $HO_2 + RO_2$ in 2007 also slightly improved: the correlation coefficient increased from 0.83 to 0.90 of OH and increased from 0.90 to 0.93 of $HO_2 + RO_2$. For the 2008 data the correlation was essentially unchanged when high RGM periods were excluded. These results indicate that OH levels are enhanced above predictions when RGM is enhanced. This is consistent with other chemistry (e.g. other halogens) coincident with the Br chemistry that leads to elevated RGM impacting the production of OH from HO_2 and RO_2.

4.5 Case study with high RGM

The concentrations of OH, O_3, RGM, and other species during two periods (16 May–21 May 2007; 12 June–17 June 2008) are shown in Fig. 9. The BM clearly under predicted OH during 16 May–18 May 2007 (Fig. 9a). Clear diurnal profiles of RGM were present during the same period, with a maximum concentration of near 250 pg m^{-3}. The RGM peaks indicate that certain levels of Br and BrO may be present during these periods. Small O_3 concentration drops also occurred with the RGM peaks, possibly a result of bromine catalyzed O_3 depletion. Despite evidence that there may be certain

ACPD
11, 12725–12762, 2011

levels of BrO present during this period, no BrO measurements from CIMS were available during this time and the BrO measurements from LP DOAS were sparse.

Figure 9b shows the early period of 2008 campaign including three days (12 June–14 June 2008) with obvious under prediction of OH. The RGM peaks during this period were the highest values in 2008 campaign with a maximum of ~80 pg m^{-3}. During this period, up to 4–5 pptv of BrO were observed by CIMS, and up to ~3 pptv of BrO were observed by LP DOAS. The gaps of BrO and HO_x measurements during 12 June–14 June 2008 were due to the extremely high wind speeds (>12 m s^{-1}). The OH predictions from BM_BrO constrained by CIMS BrO measurements are also shown in Fig. 9b. These levels of BrO were not large enough to explain the under prediction of OH. The BrO concentrations during 12 June–14 June 2008 only contribute ~10% to the OH production rate.

5 Conclusions

The median midday values of $HO_2 + RO_2$ and OH concentrations observed by CIMS were 2.7×10^8 molec cm^{-3} and 3.0×10^6 molec cm^{-3} in spring 2007, and 4.2×10^8 molec cm^{-3} and 4.1×10^6 molec cm^{-3} in summer 2008 at Summit. The BM was reasonably accurate for $HO_2 + RO_2$ ($R = 0.90$, slope = 0.87 in 2007; $R = 0.79$, slope = 0.96 in 2008) but under predicted OH ($R = 0.83$, slope = 0.72 in 2007; $R = 0.76$, slope = 0.54 in 2008). This confirmed our understanding of the dominant HO_x sources and sinks in this environment and that there may be mechanisms perturbing HO_x cycling and enhancing OH above the snow pack. Inclusion of HONO source in the model did not impact the correlation between predictions and observations of HO_x significantly and did not improve the ratio of OH to $HO_2 + RO_2$. BrO levels detected by CIMS and LP DOAS generally ranged from below detection limits to ~6 pptv and ~5 pptv, respectively. The correlation between observed and predicted $HO_2 + RO_2$ and OH from the BM_BrO_{CIMS} slightly improved relative to the BM. The model incorporating bromine chemistry brought the average hourly OH and $HO_2 + RO_2$ predictions closer

ACPD
11, 12725–12762, 2011

to the observations in 2008. This indicates that BrO at Summit impacted the HO_x levels, although most of the discrepancies between observations and models cannot be explained by the influence of detected BrO. High levels of RGM were found to be coincident with the significant under predictions of OH, and exclusion of high RGM periods significantly increased the agreement between predicted and observed OH. This is consistent with bromine chemistry and potentially other chemistry leading to elevated RGM and impacting the production OH from HO_2 and RO_2. Enhanced snow photochemistry producing H_2O_2, CH_2O and potentially other radical precursors at higher temperature may have contributed to the larger discrepancy between predicted and observed HO_x in summer 2008.

Acknowledgements. This work is financially supported by NSF GEO ATM Tropospheric Chemistry program (Grant ATM-0612279:002). We would like to thank the logistic support from NSF OPP and CH2MHill Polar Services, the transportation from Air National Guard 109th, and the permission from Greenland Home rule.

References

Ariya, P. A., Khalizov, A., and Gidas, A.: Reactions of gaseous mercury with atomic and molecular halogens: Kinetics, product studies, and atmospheric implications, J. Phys. Chem. A, 106, 7310–7320, doi:10.1021/jp020719o, 2002.

Bloss, W. J., Lee, J. D., Heard, D. E., Salmon, R. A., Bauguitte, S. J.-B., Roscoe, H. K., and Jones, A. E.: Observations of OH and HO_2 radicals in coastal Antarctica, Atmos. Chem. Phys., 7, 4171–4185, doi:10.5194/acp-7-4171-2007, 2007.

Bloss, W. J., Camredon, M., Lee, J. D., Heard, D. E., Plane, J. M. C., Saiz-Lopez, A., Bauguitte, S. J.-B., Salmon, R. A., and Jones, A. E.: Coupling of HO_x, NO_x and halogen chemistry in the antarctic boundary layer, Atmos. Chem. Phys., 10, 10187–10209, doi:10.5194/acp-10-10187-2010, 2010.

Brooks, S., Arimoto, R., Lindberg, S., and Southworth, G.: Antarctic polar plateau snow surface conversion of deposited oxidized mercury to gaseous elemental mercury with fractional long-term burial, Atmos. Environ., 42, 2877–2884, doi:10.1016/j.atmosenv.2007.05.029, 2008.

ACPD
11, 12725–12762, 2011

Brooks, S. B., Moore, C., Lew, D., Lefer, B., Huey, L. G., and Tanner, D.: Temperature and sunlight controls of mercury oxidation and deposition atop the Greenland ice sheet, Atmos. Chem. Phys. Discuss., 11, 3663–3691, doi:10.5194/acpd-11-3663-2011, 2011.

Chen, G., Davis, D., Crawford, J., Nowak, J. B., Eisele, F., Mauldin, R. L., Tanner, D., Buhr, M., Shetter, R., Lefer, B., Arimoto, R., Hogan, A., and Blake, D.: An investigation of South Pole HO_x chemistry: Comparison of model results with ISCAT observations, Geophys. Res. Lett., 28, 3633–3636, 2001.

Chen, G., Davis, D., Crawford, J., Hutterli, L. M., Huey, L. G., Slusher, D., Mauldin, L., Eisele, F., Tanner, D., Dibb, J., Buhr, M., McConnell, J., Lefer, B., Shetter, R., Blake, D., Song, C. H., Lombardi, K., and Arnoldy, J.: A reassessment of HO_x South Pole chemistry based on observations recorded during ISCAT 2000, Atmos. Environ., 38, 5451–5461, doi:10.1016/j.atmosenv.2003.07.018, 2004.

Chen, G., Huey, L. G., Crawford, J. H., Olson, J. R., Hutterli, M. A., Sjostedt, S., Tanner, D., Dibb, J., Lefer, B., Blake, N., Davis, D., and Stohl, A.: An assessment of the polar HO_x photochemical budget based on 2003 Summit Greenland field observations, Atmos. Environ., 41, 7806–7820, doi:10.1016/j.atmosenv.2007.06.014, 2007.

Crawford, J. H., Davis, D. D., Chen, G., Buhr, M., Oltmans, S., Weller, R., Mauldin, L., Eisele, F., Shetter, R., Lefer, B., Arimoto, R., and Hogan, A.: Evidence for photochemical production of ozone at the South Pole surface, Geophys. Res. Lett., 28, 3641–3644, 2001.

Davis, D., Nowak, J. B., Chen, G., Buhr, M., Arimoto, R., Hogan, A., Eisele, F., Mauldin, L., Tanner, D., Shetter, R., Lefer, B., and McMurry, P.: Unexpected high levels of NO observed at South Pole, Geophys. Res. Lett., 28, 3625–3628, 2001.

Dibb, J. E. and Jaffrezo, J. L.: Air-snow exchange investigations at Summit, Greenland: An overview, J. Geophys. Res.-Oceans, 102, 26795–26807, 1997.

Dibb, J. E., Talbot, R. W., Munger, J. W., Jacob, D. J., and Fan, S. M.: Air-snow exchange of HNO_3 and NO_y at Summit, Greenland, J. Geophys. Res.-Atmos., 103, 3475–3486, 1998.

Dibb, J. E., Arsenault, M., Peterson, M. C., and Honrath, R. E.: Fast nitrogen oxide photochemistry in Summit, Greenland snow, Atmos. Environ., 36, 2501–2511, 2002.

Dibb, J. E., Huey, L. G., Slusher, D. L., and Tanner, D. J.: Soluble reactive nitrogen oxides at South Pole during ISCAT 2000, Atmos. Environ., 38, 5399–5409, doi:10.1016/j.atmosenv.2003.01.001, 2004.

Donohoue, D. L., Bauer, D., Cossairt, B., and Hynes, A. J.: Temperature and pressure dependent rate coefficients for the reaction of Hg with Br and the reaction of Br with Br: A

ACPD
11, 12725–12762, 2011

pulsed laser photolysis-pulsed laser induced fluorescence study, J. Phys. Chem. A, 110, 6623–6632, doi:10.1021/jp054688j, 2006.
Faïn, X., Ferrari, C. P., Dommergue, A., Albert, M., Battle, M., Arnaud, L., Barnola, J.-M., Cairns, W., Barbante, C., and Boutron, C.: Mercury in the snow and firn at Summit Station, Central Greenland, and implications for the study of past atmospheric mercury levels, Atmos. Chem. Phys., 8, 3441–3457, doi:10.5194/acp-8-3441-2008, 2008.
Grannas, A. M., Jones, A. E., Dibb, J., Ammann, M., Anastasio, C., Beine, H. J., Bergin, M., Bottenheim, J., Boxe, C. S., Carver, G., Chen, G., Crawford, J. H., Dominé, F., Frey, M. M., Guzmán, M. I., Heard, D. E., Helmig, D., Hoffmann, M. R., Honrath, R. E., Huey, L. G., Hutterli, M., Jacobi, H. W., Klàn, P., Lefer, B., McConnell, J., Plane, J., Sander, R., Savarino, J., Shepson, P. B., Simpson, W. R., Sodeau, J. R., von Glasow, R., Weller, R., Wolff, E. W., and Zhu, T.: An overview of snow photochemistry: evidence, mechanisms and impacts, Atmos. Chem. Phys., 7, 4329–4373, doi:10.5194/acp-7-4329-2007, 2007.
Haman, C., Lefer, B., Dibb, J. E., and Clements, C.: Evidence for a mid- to upper-tropospheric source of bromide reaching Summit, Atmos. Chem. Phys. Discuss., in preparation, 2011.
Hammer, C. U., Clausen, H. B., and Dansgaard, W.: Greenland ice-sheet evidence of post-glacial volcanism and its climatic impact, Nature, 288, 230–235, 1980.
Hausmann, M. and Platt, U.: Spectroscopic measurement of bromine oxide and ozone in the high Arctic during polar sunrise experiment 1992, J. Geophys. Res.-Atmos., 99, 25399–25413, 1994.
Helmig, D., Boulter, J., David, D., Birks, J. W., Cullen, N. J., Steffen, K., Johnson, B. J., and Oltmans, S. J.: Ozone and meteorological Summit, Greenland, boundary-layer conditions at during 3–21 June 2000, Atmos. Environ., 36, 2595–2608, 2002.
Helmig, D., Johnson, B. J., Warshawsky, M., Morse, T., Neff, W. D., Eisele, F., and Davis, D. D.: Nitric oxide in the boundary-layer at South Pole during the Antarctic Tropospheric Chemistry Investigation (ANTCI), Atmos. Environ., 42, 2817–2830, doi:10.1016/j.atmosenv.2007.03.061, 2008.
Honrath, R. E., Peterson, M. C., Guo, S., Dibb, J. E., Shepson, P. B., and Campbell, B.: Evidence of NO_x production within or upon ice particles in the Greenland snowpack, Geophys. Res. Lett., 26, 695–698, 1999.
Honrath, R. E., Lu, Y., Peterson, M. C., Dibb, J. E., Arsenault, M. A., Cullen, N. J., and Steffen, K.: Vertical fluxes of NO_x, HONO, and HNO_3 above the snowpack at Summit, Greenland, Atmos. Environ., 36, 2629–2640, 2002.

ACPD
11, 12725–12762, 2011

Huey, L. G., Tanner, D. J., Slusher, D. L., Dibb, J. E., Arimoto, R., Chen, G., Davis, D., Buhr, M. P., Nowak, J. B., Mauldin, R. L., Eisele, F. L., and Kosciuch, E.: CIMS measurements of HNO_3 and SO_2 at the South Pole during ISCAT 2000, Atmos. Environ., 38, 5411–5421, doi:10.1016/j.atmosenv.2004.04.037, 2004.

Huey, L. G., Hanson, D. R., and Howard, C. J.: Reactions of SF_6^- and I^- with atmospheric trace gases, J. Phys. Chem., 99, 5001–5008, 1995.

Hutterli, M. A., Rothlisberger, R., and Bales, R. C.: Atmosphere-to-snow-to-firn transfer studies of HCHO at Summit, Greenland, Geophys. Res. Lett., 26, 1691–1694, 1999.

Hutterli, M. A., McConnell, J. R., Stewart, R. W., Jacobi, H. W., and Bales, R. C.: Impact of temperature-driven cycling of hydrogen peroxide (H_2O_2) between air and snow on the planetary boundary layer, J. Geophys. Res.-Atmos., 106, 15395–15404, 2001.

Hutterli, M. A., McConnell, J. R., Chen, G., Bales, R. C., Davis, D. D., and Lenschow, D. H.: Formaldehyde and hydrogen peroxide in air, snow and interstitial air at South Pole, Atmos. Environ., 38, 5439–5450, doi:10.1016/j.atmosenv.2004.06.003, 2004.

Jefferson, A., Tanner, D. J., Eisele, F. L., Davis, D. D., Chen, G., Crawford, J., Huey, J. W., Torres, A. L., and Berresheim, H.: OH photochemistry and methane sulfonic acid formation in the coastal Antarctic boundary layer, J. Geophys. Res.-Atmos., 103, 1647–1656, 1998.

Jones, A. E., Wolff, E. W., Salmon, R. A., Bauguitte, S. J.-B., Roscoe, H. K., Anderson, P. S., Ames, D., Clemitshaw, K. C., Fleming, Z. L., Bloss, W. J., Heard, D. E., Lee, J. D., Read, K. A., Hamer, P., Shallcross, D. E., Jackson, A. V., Walker, S. L., Lewis, A. C., Mills, G. P., Plane, J. M. C., Saiz-Lopez, A., Sturges, W. T., and Worton, D. R.: Chemistry of the Antarctic Boundary Layer and the Interface with Snow: an overview of the CHABLIS campaign, Atmos. Chem. Phys., 8, 3789–3803, doi:10.5194/acp-8-3789-2008, 2008.

Kim, S., Huey, L. G., Stickel, R. E., Tanner, D. J., Crawford, J. H., Olson, J. R., Chen, G., Brune, W. H., Ren, X., Lesher, R., Wooldridge, P. J., Bertram, T. H., Perring, A., Cohen, R. C., Lefer, B. L., Shetter, R. E., Avery, M., Diskin, G., and Sokolik, I.: Measurement of HO_2NO_2 in the free troposphere during the intercontinental chemical transport experiment – North America 2004, J. Geophys. Res.-Atmos., 112, D12s01, doi:10.1029/2006jd007676, 2007.

Liao, J., Sihler, H., Huey, L. G., Neuman, J. A., Tanner, D. J., Friess, U., Platt, U., Flocke, F. M., Orlando, P. B. Shepson, J. J., Beine, H. J., Weinheimer, A. J., Sjostedt, S. J., Nowak, J.B., Knapp, D. J., Staebler, R. M., Zheng, W., Sander, R., Hall, S. R., and Ullman, K.: A comparison of Arctic BrO measurements by chemical ionization mass spectrometry (CIMS) and long path-differential optical absorption spectroscopy (LP-DOAS), J. Geophys. Res.,

ACPD
11, 12725–12762, 2011

116, D00R02, doi:10.1029/2010JD014788, 2011a.
Liao, J., Huey, L.G., Tanner, D. J., Neuman, J.A., Flocke, F. M., Orlando, J. J., Nowak, J. B., Hall, S. R., Smith, J. N., Wang, Y., and Koo, J.: Observations of specific inorganic bromine species (HOBr, BrO, Br_2 and BrCl) at Barrow, AK, J. Geophys. Res, submitted, 2011b.
Mahajan, A. S., Oetjen, H., Lee, J. D., Saiz-Lopez, A., McFiggans, G. B., and Plane, J. M. C.: High bromine oxide concentrations in the semi-polluted boundary layer, Atmos. Environ., 43, 3811–3818, doi:10.1016/j.atmosenv.2009.05.033, 2009.
Mauldin, R. L., Eisele, F. L., Tanner, D. J., Kosciuch, E., Shetter, R., Lefer, B., Hall, S. R., Nowak, J. B., Buhr, M., Chen, G., Wang, P., and Davis, D.: Measurements of OH, H_2SO_4, and MSA at the South Pole during ISCAT, Geophys. Res. Lett., 28, 362-9-3632, 2001.
Mauldin, R. L., Kosciuch, E., Henry, B., Eisele, F. L., Shetter, R., Lefer, B., Chen, G., Davis, D., Huey, G., and Tanner, D.: Measurements of OH, $HO_2 + RO_2$, H_2SO_4, and MSA at the south pole during ISCAT 2000, Atmos. Environ., 38, 5423–5437, doi:10.1016/j.atmosenv.2004.06.031, 2004.
Mauldin, R., Kosciuch, E., Eisele, F., Huey, G., Tanner, D., Sjostedt, S., Blake, D., Chen, G., Crawford, J., and Davis, D.: South Pole Antarctica observations and modeling results: New insights on HO_x radical and sulfur chemistry, Atmos. Environ., 44, 572–581, doi:10.1016/j.atmosenv.2009.07.058, 2010.
Mayewski, P. A. and Bender, M.: The GISP2 ice core record- paleoclimate highlights, Rev. Geophys., 33, 1287–1296, 1995.
Neuman, J. A., Nowak, J. B., Huey, L. G., Burkholder, J. B., Dibb, J. E., Holloway, J. S., Liao, J., Peischl, J., Roberts, J. M., Ryerson, T. B., Scheuer, E., Stark, H., Stickel, R. E., Tanner, D. J., and Weinheimer, A.: Bromine measurements in ozone depleted air over the Arctic Ocean, Atmos. Chem. Phys., 10, 6503–6514, doi:10.5194/acp-10-6503-2010, 2010.
Read, K. A., Mahajan, A. S., Carpenter, L. J., Evans, M. J., Faria, B. V. E., Heard, D. E., Hopkins, J. R., Lee, J. D., Moller, S. J., Lewis, A. C., Mendes, L., McQuaid, J. B., Oetjen, H., Saiz-Lopez, A., Pilling, M. J., and Plane, J. M. C.: Extensive halogen-mediated ozone destruction over the tropical Atlantic Ocean, Nature, 453, 1232–1235, doi:10.1038/nature07035, 2008.
Ren, X. R., Olson, J. R., Crawford, J. H., Brune, W. H., Mao, J. Q., Long, R. B., Chen, Z., Chen, G., Avery, M. A., Sachse, G. W., Barrick, J. D., Diskin, G. S., Huey, L. G., Fried, A., Cohen, R. C., Heikes, B., Wennberg, P. O., Singh, H. B., Blake, D. R., and Shetter, R. E.: HO_x chemistry during INTEX-A 2004: Observation, model calculation, and comparison with previous studies, J. Geophys. Res.-Atmos., 113, D05310, doi:10.1029/2007jd009166, 2008.

ACPD
11, 12725–12762, 2011

Ryerson, T. B., Williams, E. J., and Fehsenfeld, F. C.: An efficient photolysis system for fast-response NO_2 measurements, J. Geophys. Res.-Atmos., 105, 26447–26461, 2000.
Saiz-Lopez, A., Shillito, J. A., Coe, H., and Plane, J. M. C.: Measurements and modelling of I_2, IO, OIO, BrO and NO_3 in the mid-latitude marine boundary layer, Atmos. Chem. Phys., 6, 1513–1528, doi:10.5194/acp-6-1513-2006, 2006.
Saiz-Lopez, A., Mahajan, A. S., Salmon, R. A., Bauguitte, S. J. B., Jones, A. E., Roscoe, H. K., and Plane, J. M. C.: Boundary layer halogens in coastal Antarctica, Science, 317, 348–351, doi:10.1126/science.1141408, 2007.
Sander, S. P, Friedl, R. R., Golden, D. M., Kurylo, M. J., Moortgat, Keller-Rudek, H., G. K., Wine, P. H., Ravishankara, A. R., Kolb, C. E., Molina, M. J., Finlayson-Pitts, B., Huie, R. E., and Orkin, V. L: Chemical Kinetics and Photochemical Data for Use in Atmospheric Studies Evaluation Number 15, JPL Publ. 06-2, NASA Jet Propulsion Laboratory, California Institute of Technology, Pasadena, CA, 2006.
Shetter, R. E. and Muller, M.: Photolysis frequency measurements using actinic flux spectroradiometry during the PEM-Tropics mission: Instrumentation description and some results, J. Geophys. Res.-Atmos., 104, 5647–5661, 1999.
Sjostedt, S. J.: Investigation of photochemistry at high latitudes: comparison of model predictions to measurements of short lived species, Ph.D thesis, Georgia Institute of Technology, Atlanta, 2006.
Sjostedt, S. J., Huey, L. G., Tanner, D. J., Peischl, J., Chen, G., Dibb, J. E., Lefer, B., Hutterli, M. A., Beyersdorf, A. J., Blake, N. J., Blake, D. R., Sueper, D., Ryerson, T., Burkhart, J., and Stohl, A.: Observations of hydroxyl and the sum of peroxy radicals at Summit, Greenland during summer 2003, Atmos. Environ., 41, 5122–5137, doi:10.1016/j.atmosenv.2006.06.065, 2007.
Slusher, D. L., Pitteri, S. J., Haman, B. J., Tanner, D. J., and Huey, L. G.: A chemical ionization technique for measurement of pernitric acid in the upper troposphere and the polar boundary layer, Geophys. Res. Lett., 28, 3875–3878, 2001.
Slusher, D. L., Huey, L. G., Tanner, D. J., Chen, G., Davis, D. D., Buhr, M., Nowak, J. B., Eisele, F. L., Kosciuch, E., Mauldin, R. L., Lefer, B. L., Shetter, R. E., and Dibb, J. E.: Measurements of pernitric acid at the South Pole during ISCAT 2000, Geophys. Res. Lett., 29, doi:10.1029/2002gl015703, 2011. 2002.
Streit, G. E.: Negative-ion chemistry and the electron-affinity of SF_6, J. Chem. Phys., 77, 826–833, 1982.

ACPD
11, 12725–12762, 2011

Stutz, J. and Platt, U.: Improving long-path differential optical absorption spectroscopy with a quartz-fiber mode mixer, Appl. Optics, 36, 1105–1115, 1997.

Stutz, J., Thomas, J. L., Hurlock, S. C., Schneider, M., von Glasow, R., Piot, M., Gorham, K., Burkhart, J. F., Ziemba, L., Dibb, J. E., and Lefer, B. L.: Longpath DOAS observations of surface BrO at Summit, Greenland, Atmos. Chem. Phys. Discuss., 11, 6707–6736, doi:10.5194/acpd-11-6707-2011, 2011.

Swanson, A. L., Blake, N. J., Dibb, J. E., Albert, M. R., Blake, D. R., and Rowland, F. S.: Photochemically induced production of CH_3Br, CH_3I, C_2H_5I, ethene, and propene within surface snow at Summit, Greenland, Atmos. Environ., 36, 2671–2682, 2002.

Tanner, D. J., Jefferson, A., and Eisele, F. L.: Selected ion chemical ionization mass spectrometric measurement of OH, J. Geophys. Res.-Atmos., 102, 6415–6425, 1997.

Thomas, J. L., Stutz, J., Lefer, B., Huey, L. G., Toyota, K., Dibb, J. E., and von Glasow, R.: Modeling chemistry in and above snow at Summit, Greenland – Part 1: Model description and results, Atmos. Chem. Phys. Discuss., 10, 30927–30970, doi:10.5194/acpd-10-30927-2010, 2010.

Thomas, J. L., Stutz, J., Dibb, J. E., Huey, L. G., Lefer, B., and von Glasow, R.: Modeling halogen chemistry in and above snow at Summit, Greenland – Part 2: Radical Chemistry and Sensitivity Studies, Atmos. Chem. Phys. Discuss., in preparation, 2011.

Tuckermann, M., Ackermann, R., Golz, C., LorenzenSchmidt, H., Senne, T., Stutz, J., Trost, B., Unold, W., and Platt, U.: DOAS-observation of halogen radical-catalysed arctic boundary layer ozone destruction during the ARCTOC-campaigns 1995 and 1996 in Ny-Alesund, Spitsbergen, Tellus B, 49, 533–555, 1997.

Yang, J., Honrath, R. E., Peterson, M. C., Dibb, J. E., Sumner, A. L., Shepson, P. B., Frey, M., Jacobi, H. W., Swanson, A., and Blake, N.: Impacts of snowpack emissions on deduced levels of OH and peroxy radicals at Summit, Greenland, Atmos. Environ., 36, 2523–2534, 2002.

Ziemba, L. D., Dibb, J. E., Griffin, R. J., Huey, L. G., and Beckman, P.: Observations of particle growth at a remote, Arctic site, Atmos. Environ., 44, 1649–1657, doi:10.1016/j.atmosenv.2010.01.032, 2010.

ACPD

11, 12725–12762, 2011

Table 1. Summary of the measurements at Summit, Greenland 2007–2008.

Species and parameters	Instrument	Uncertainty	Institution	Reference
O_3	UV absorption ozone analyzer	< ±5%	Ga. Tech	
NO	Chemilluminesent gas analyzer	±10%	Ga. Tech	Ryerson et al. (2000)
CO	Canister/GC	< ±5%	UCI	Swanson et al. (2002)
CH_4	Canister/GC	< ±5%	UCI	Swanson et al. (2002)
NMHC	Canister/GC	< ±5%	UCI	Swanson et al. (2002)
OH	CIMS	±30%	Ga. Tech	Sjostedt et al. (2007)
$HO_2 + RO_2$	CIMS	±35%	Ga. Tech	Sjostedt et al. (2007)
BrO	CIMS	±30% –36%	Ga. Tech	Liao et al. (2011a)
BrO	DOAS	±10%	UCLA	Stutz et al. (2011)
SMPS_N	SMPS/CPC	±10%	UNH	Ziemba et al. (2010)
SMPS_S	SMPS/CPC	±10%	UNH	Ziemba et al. (2010)
GEM	Tekran	±2%	NOAA	Brooks et al. (2011)
RGM	Tekran	±5%	NOAA	Brooks et al. (2011)
FPM	Tekran	±5%	NOAA	Brooks et al. (2011)
HNO_3	Mist Chamber	±15% –20%	UNH	Dibb et al. (1998)
Soluble Bromine	Mist Chamber	±15% –20%	UNH	Dibb et al. (1998)
HONO	Mist Chamber	±15% –20%	UNH	Dibb et al. (1998)
Actinic Flux	SAFS	±10%	U. Houston	Shetter et al. (1999)
Temperature	F-Thermocouples	±0.5˚C	U. Houston	Haman et al. (2011)
WS/WD	AWS/Digital compass		U. Houston	Haman et al. (2011)

ACPD
11, 12725–12762, 2011

Table 2. Bromine reactions included in the HO_x model.

Reaction number	Reactions	Reaction rate coefficient k (cm^3 $molec^{-1}$ s^{-1} or s^{-1})	$k(T = 250\,K)$ (cm^3 $molec^{-1}$ s^{-1} or s^{-1})
1	$Br + O_3 \rightarrow BrO + O_2$	$1.7 \times 10^{-11} exp(-800/T)$	6.9×10^{-13}
2	$BrO + HO_2 \rightarrow HOBr + O_2$	$4.5 \times 10^{-12} exp(460/T)$	2.8×10^{-11}
3a	$BrO + BrO \rightarrow 2Br + O_2$	$2.4 \times 10^{-12} exp(40/T)$	2.8×10^{-12}
3b	$\rightarrow Br_2 + O_2$	$2.8 \times 10^{-14} exp(860/T)$	8.7×10^{-13}
4	$BrO + NO \rightarrow Br + NO_2$	$8.8 \times 10^{-12} exp(260/T)$	2.5×10^{-11}
5	$BrO + NO_2 + M \rightarrow BrONO_2 + M$	$k_0 = 5.2 \times 10^{-31} exp(T/300)^{-3.2}$ $k_\infty = 6.9 \times 10^{-12} exp(T/300)^{-2.9}$	5.3×10^{-12}
6	$Br + CH_2O \rightarrow HBr + HCO$	1.7×10^{-11} $exp(-800/T)$	6.9×10^{-13}
7	$BrO + h\nu \rightarrow Br + O$	0.06–0.08 (at noon)	
8	$HOBr + h\nu \rightarrow Br + OH$	$3 \times 10^{-3} - 4 \times 10^{-3}$ (at noon)	
9	Uptake of HOBr on heterogeneous surface	$\sim 1 \times 10^{-4}$	

ACPD
11, 12725–12762, 2011

Table 3. Photochemical species concentrations and parameters in the mid-day (10:00–15:00 WGST) at Summit, Greenland in 2007–2008. (Note: HO_x predictions are from the base model.)

Species	Year 2007 (13 May–13 June)		Year 2008 (10 June–8 July)	
	Median	Average	Median	Average
OH (10^6 molec cm^{-3})	3.0	3.1	4.1	4.6
$HO_2 + RO_2$ (10^8 molec cm^{-3})	2.7	3.3	4.2	4.4
OH pred (10^6 molec cm^{-3})	2.4	2.6	3.7	3.8
$HO_2 + RO_2$pred (10^8 molec cm^{-3})	3.0	3.2	4.6	4.6
NO (pptv)	12.8	17.2	8.6	11.4
O_3 (ppbv)	54.6	55.3	47.3	47.9
BrO_{LPDOAS} (pptv)	1.5	1.6	1.0	0.9
BrO_{CIMS} (pptv)	1.8	2.0	1.5	2.0
RGM(pg m^{-3})	41.8	64.8	7.2	9.6
HNO_3 (pptv)	12.9	15.9	5.5	11.5
HONO (pptv)	6.5	7.3	4.7	5.8
$J(O^1D)$ (10^{-5} s^{-1})	2.2	2.3	3.3	3.3
JNO_2 (s^{-1})	0.014	0.014	0.016	0.016
Temperature (°C)	−19.5	−18.2	−10.7	−10.6

ACPD
11, 12725–12762, 2011

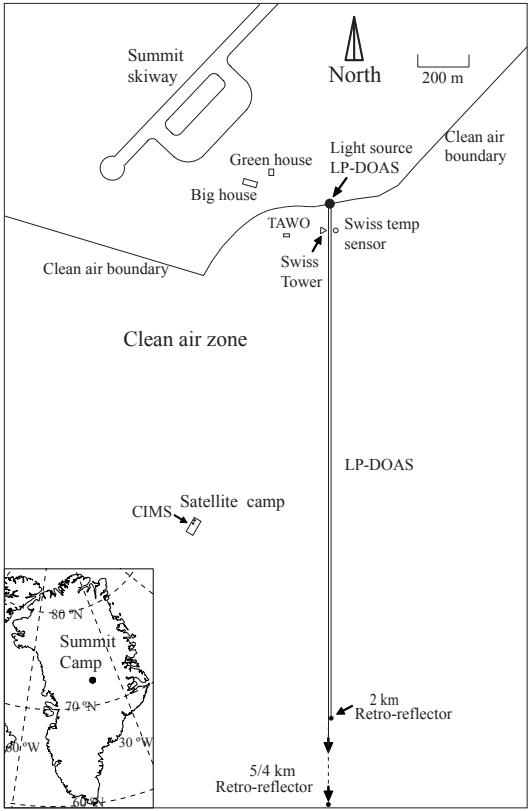

Fig. 1. The layout of the CIMS and LP-DOAS instruments in the Summit campaign.

ACPD
11, 12725–12762, 2011

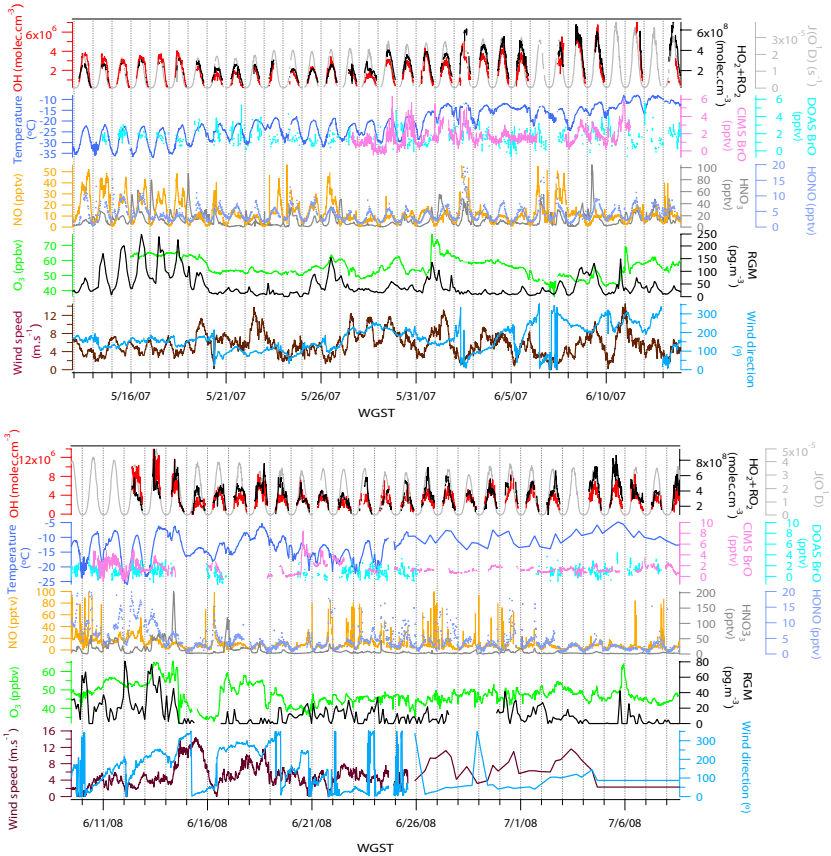

Fig. 2. Time series of measurements of $HO_2 + RO_2$, OH, $J(O^1D)$, BrO, temperature, NO, HNO_3, HONO, O_3, RGM, wind speeds and directions on a 10 min time base in spring 2007 (top panel) and summer 2008 (bottom panel) Summit campaign.

ACPD
11, 12725–12762, 2011

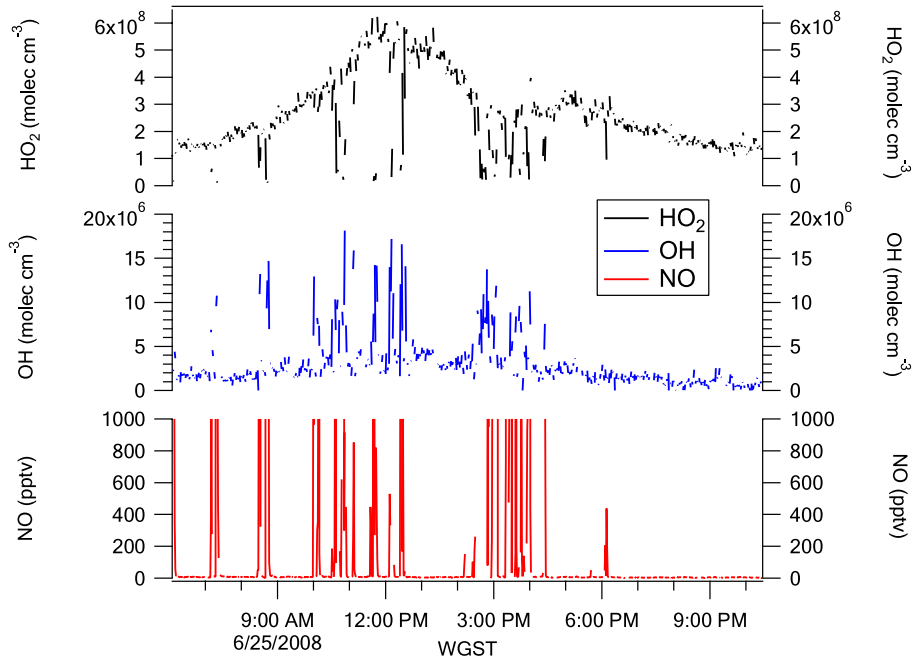

Fig. 3. An example of elevated OH and depleted HO_2 at high NO conditions.

ACPD
11, 12725–12762, 2011

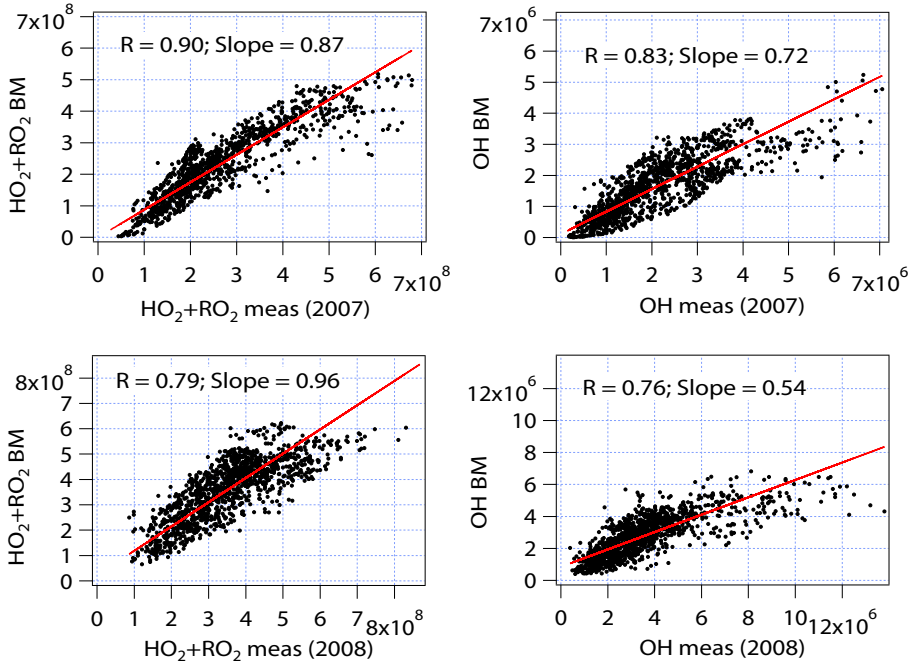

Fig. 4. $HO_2 + RO_2$ and OH predictions from the base mode (BM) plotted versus the observations in 2007 and 2008. The data are average on a 10 min time base. The correlation coefficient (R) and the slope from an equally weighted bivariate regression (red line) for each panel are also denoted in the figure. The units are molec cm^{-3}.

ACPD
11, 12725–12762, 2011

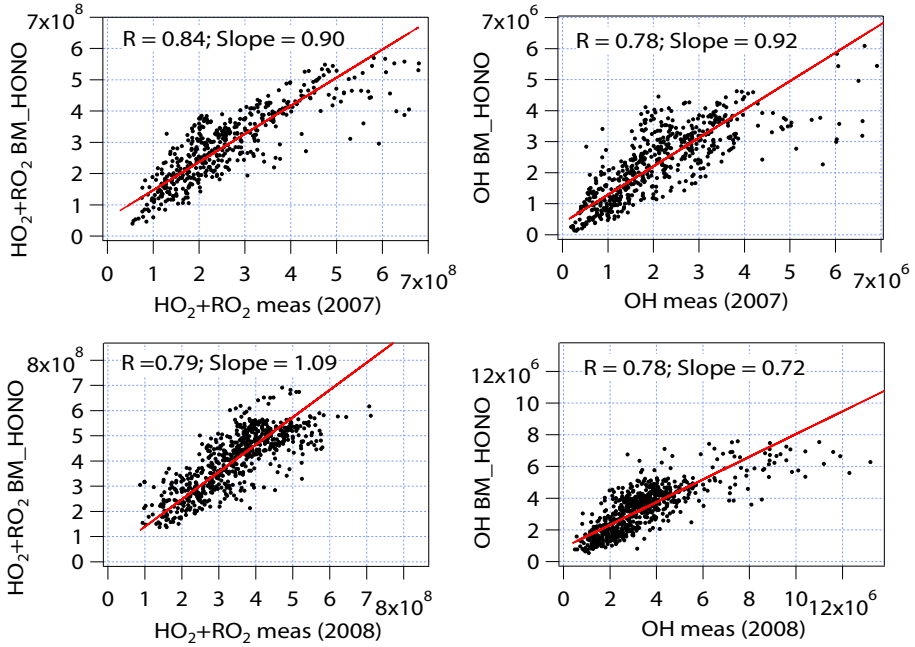

Fig. 5. $HO_2 + RO_2$ and OH predictions from the base model constrained to HONO measurements (BM_HONO) plotted versus the observations in 2007 and 2008. The data are average on a 10 min time base. The correlation coefficient (R) and the slope from an equally weighted bivariate regression (red line) for each panel are also denoted in the figure. The units are molec cm^{-3}.

ACPD
11, 12725–12762, 2011

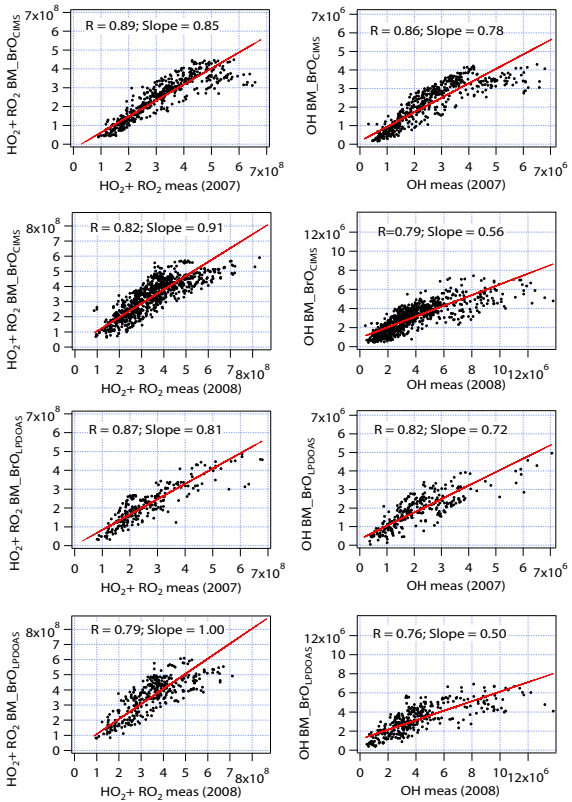

Fig. 6. $HO_2 + RO_2$ and OH predictions from the base model incorporating bromine chemistry constrained by BrO measurements by CIMS (BM_BrO_{CIMS}) and LPDOAS (BM_BrO_{LPDOAS}) plotted versus the observations in 2007 and 2008. The data are average on a 10 min time base. The correlation coefficient (R) and the slope from an equally weighted bivariate regression (red line) for each panel are also denoted in the figure. The units are molec cm^{-3}.

ACPD
11, 12725–12762, 2011

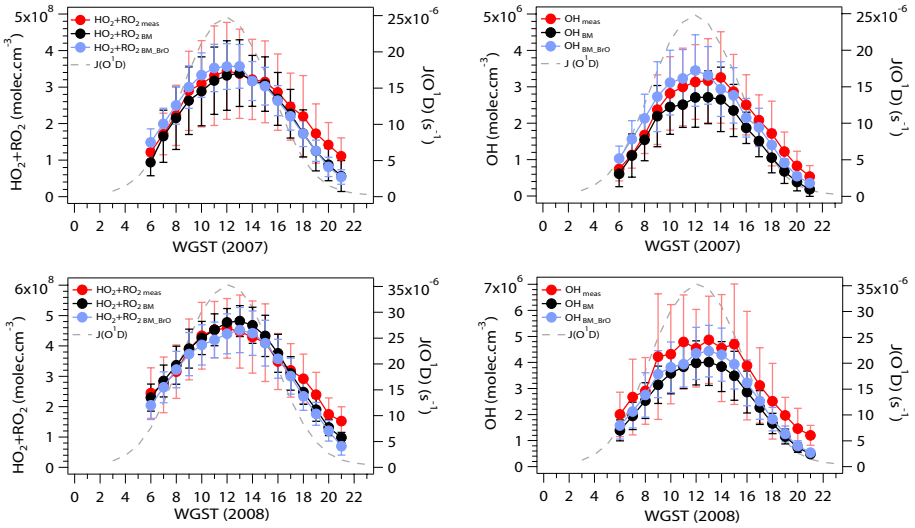

Fig. 7. The average diurnal profiles of hourly OH and $HO_2 + RO_2$ observations (red dots and line) and predictions from the BM (black dots and line) and BM_BrO_{CIMS} (blue dots and line), and diurnal profile of $J(O^1D)$ (gray dash line) in spring 2007 and summer 2008. The error bars (red) of the observations are the overall uncertainties including the measurement uncertainties and ambient fluctuations. The error bars (gray and blue) of the predictions are the propagated uncertainties from the model input uncertainties and variations.

ACPD
11, 12725–12762, 2011

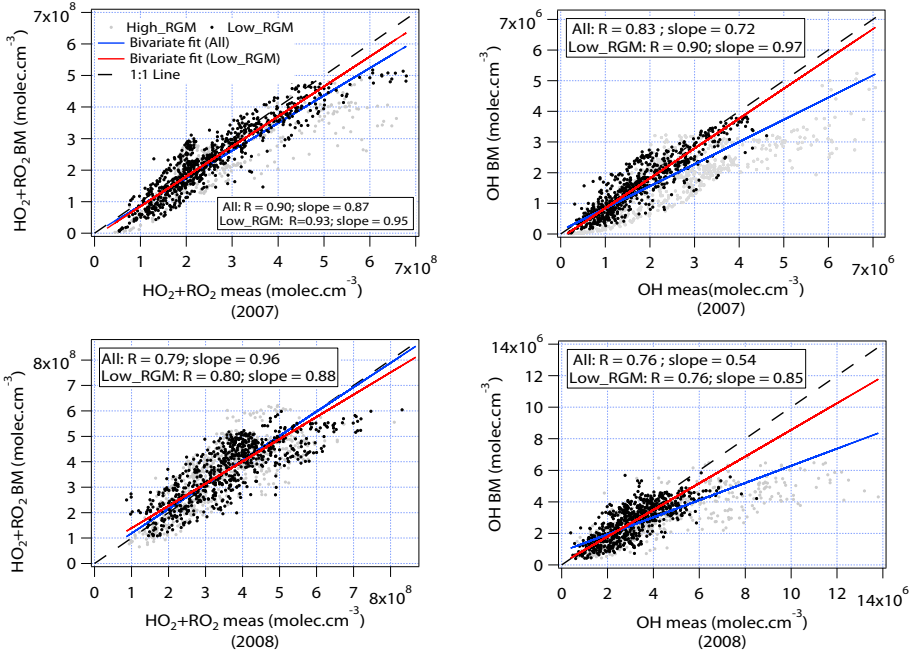

Fig. 8. The correlation plots of observed and predicted OH and $HO_2 + RO_2$ from BM at low RGM conditions (black dots) and at high RGM conditions (gray dots) in 2007 and 2008. "All" represents the total data including low RGM and high RGM conditions. Equally weighted bivariate regressions are applied to all the data (blue line) and the data at low RGM conditions (red line), respectively. The relevant correlation coefficients and slopes are provided in the figure.

ACPD
11, 12725–12762, 2011

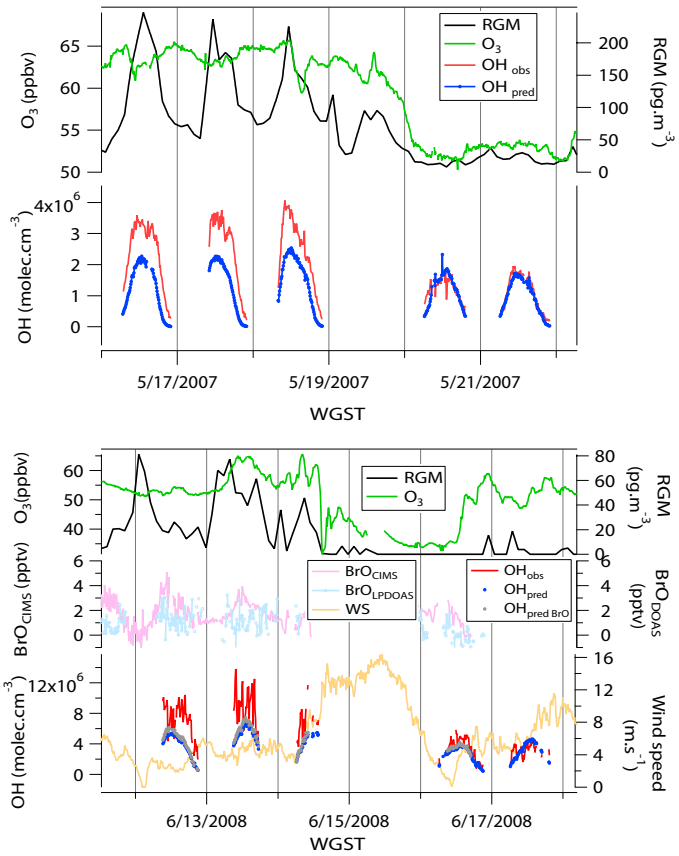

Fig. 9. (a): Observations of RGM, O_3 and OH, and predictions of OH when enhanced RGM were observed in 2007 (16 May–21 May 2007); **(b)**: The observations of RGM, O_3, OH, wind speeds, BrO by CIMS and DOAS, and the predictions of OH from the BM and BM_BrO when enhanced RGM were observed in 2008 (11 June–17 June 2008).

ACPD
11, 12725–12762, 2011